A Heme *c*-Peptide Model System for the Resonance Raman Study of *c*-Type Cytochromes: Characterization of the Solvent-Dependence of Peptide–Histidine–Heme Interactions

Samya Othman, Antoine Le Lirzin,[‡] and Alain Desbois[*]

Section de Biophysique des Protéines et des Membranes, Département de Biologie Cellulaire et Moléculaire, Unité de Recherche Associée au CNRS 1290, Centre d'Etudes de Saclay, F-91191 Gif-sur-Yvette Cedex, France

Received February 22, 1993; Revised Manuscript Received June 8, 1993[⊗]

ABSTRACT: The visible absorption and Soret-excited resonance Raman spectra of ferrous microperoxidase-8 [MP8(II)], an octapeptide containing a heme *c*, are reported. These spectroscopies indicate that MP8(II), dissolved in aqueous buffered solutions, forms low-spin six-coordinated complexes in the 7–14 pH range. Intermolecular bonding interactions of MP8(II) in water account for this behavior. On the contrary, when the hemopeptide is dispersed in aqueous solutions containing detergent or an alcohol, the spectroscopic data show that the iron atom of MP8(II) is essentially high-spin five-coordinated in accordance with a monomeric structure of MP8(II). In addition to a high-spin signature to the heme skeletal modes, the high-frequency regions of resonance Raman spectra characterize an electronic influence of the thioether bridges on the frequency of stretching modes of C_β-C_β bonds (ν_2, ν_{11}, and ν_{29}). On the other hand, the low-frequency Raman spectra of monomeric MP8(II) at pH 7.5 present significant differences in the 150–250-cm^{-1} regions depending upon the solvent composition (pH, presence or absence of detergent, alcohol). These effects are attributed to frequency variations of the Fe–N(His)-involving mode which indicate changes in the H-bonding interactions of the axial His and therefore solvent-dependent changes of the octapeptide conformation. Our resonance Raman data further show that the axial His of monomeric MP8(II) could be totally deprotonated in aqueous cetyltrimethylammonium bromide solution at very alkaline pH (pK_a = 13.3). The vibrational data (100–1700 cm^{-1}) obtained for the various monomeric forms of MP8(II) are expected to be useful for determining the heme structure and environment in reduced *c*′-type cytochromes. Comparisons of resonance Raman data with X-ray crystallographic data available for different hemoproteins allow us to evaluate the ionization and H-bonding states of the His bound to the high-spin five-coordinated hemes. These data are discussed in terms of proximal influence of protein–His–heme interactions on the determination and the regulation of a particular biological function.

The *c*-type cytochromes are wide-spread hemoproteins which play essential roles in living organisms. These electron carriers are, indeed, involved in electron transfers of respiratory chains of eucaryotic organisms, of photosynthetic processes in green algaes and plants, or of anaerobic dark reactions of nitrate or sulphate reduction of bacteria (Lemberg & Barrett, 1973). Their midpoint redox potentials vary largely between −350 and +450 mV (Meyer & Kamen, 1982) and are tuned so that they can take their appropriate thermodynamic places in the biological electron-transfer pathway(s) in which they are involved. The nature of axial ligands of the heme iron and the possibility of H-bonding or deprotonation of these ligands, the polarity of the heme environment, and the electrostatic charge of the protein are factors which seem to largely contribute to this variation of biological activity (Harbury et al., 1965; Kassner, 1973; Stellwagen, 1978; Mashiko et al., 1979; Valentine et al., 1979; Schejter et al., 1982). X-ray crystallography is obviously the most powerful technique to estimate the relative contributions of these factors on the redox properties. However, due to difficulties of protein crystallization, the number of three-dimensional structures of *c*-type cytochromes, solved at a sufficiently high resolution, is still relatively limited (Bushnell et al., 1990, and references therein). On the other hand, spectroscopic techniques have been used to obtain this structural information in solution. Nuclear magnetic resonance, electron paramagnetic resonance, and magnetic circular dichroism have been applied with large success (Moore & Williams, 1980; Senn & Wüthrich, 1985; Brautigan et al., 1977; Vickery et al., 1976; Greenwood et al., 1984; Simpkin et al., 1989). However, these complementary methods have sometimes revealed either a limitation originating from the state of the heme iron (oxidation and/or spin state(s)) or an ambiguity in the interpretation of spectral data. Resonance Raman (RR)[1] spectroscopy has also been used for the study of cytochromes *c* (Strekas & Spiro, 1972; Kitagawa et al., 1977; Shelnutt et al., 1981; Cartling, 1983). This sensitive technique can, in principle, yield direct information about the axial ligands and the conformation and environment of the heme–iron complex inside the proteins (Spiro, 1985; Kitagawa & Ozaki, 1987; Desbois et al., 1984b). In studies of structure–function relationships of cyt *c*, RR spectroscopy of chemically-modified proteins (Ikeda-Saito et al., 1975),

[*] To whom correspondence should be addressed.

[‡] Present address: Laboratoire de Chimie des Solides, Université de Bordeaux I, 351 Cours de la Libération, 33405 Talence Cedex, France.

[⊗] Abstract published in *Advance ACS Abstracts,* August 15, 1993.

[1] Abbreviations: MP8, microperoxidase-8; cyt, cytochrome; Hb, hemoglobin; Lb, leghemoglobin; Mb, myoglobin; CcP, cytochrome *c* peroxidase; HRP, horseradish peroxidase; TP, turnip peroxidase; RR, resonance Raman; CTABr, cetyltrimethylammonium bromide; EtOH, ethanol; NaDS, sodium dodecyl sulfate; ProtoP, protoporphyrin IX; MesoP, mesoporphyrin IX; HematoP, hematoporphyrin IX; DeuteroP, deuteroporphyrin IX; OEP, octaethylporphyrin; His, histidine; HisOMe, histidine methyl ester; *N*-BocHis, N_α-(*tert*-butoxycarbonyl)histidine; His$^-$, histidinate; ImH, imidazole; Im$^-$, imidazolate; 2MeImH, 2-methylimidazole; 2MeIm$^-$, 2-methylimidazolate; HS, high-spin; LS, low-spin.

0006-2960/93/0432-9781$04.00/0

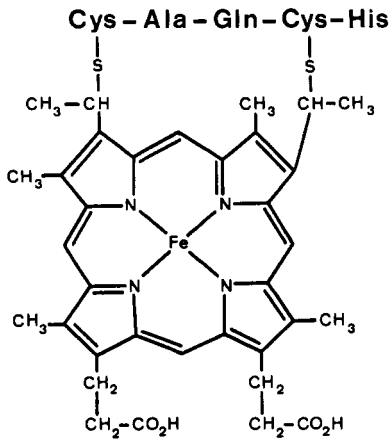

FIGURE 1: Chemical structure of microperoxidase-8.

ligated derivatives (Kitagawa et al., 1975), and more recently, mutated proteins (Hildebrandt et al., 1991) has also proven useful in several ways. However, in order to accede to specific structural information, it is necessary to compare the spectral data obtained for the hemoproteins to those determined from relevant model compounds. A number of reports have described the RR spectra of model systems for the active sites of hemoproteins. Iron–mesoporphyrin (Fe–MesoP) and iron–octaethylporphyrin (Fe–OEP) have often been used as analogs to the *c*-type heme. Nevertheless, these metalloporphyrins do not provide a strict chemical analogy with the natural heme *c*, since their peripheral compositions are different; a major problem for the interpretation of RR data is the significant influence of the heme peripheral groups on the porphyrin vibrational modes (Choi et al., 1982, 1983; Desbois et al., 1984a). Moreover, Fe–MesoP and Fe–OEP are inappropriate metalloporphyrins for the preparation of heme compounds with different axial ligands, a situation that is frequently found for *c*-type cytochromes. Therefore, in order to obtain a better approach of RR spectra of *c*-type cytochromes, we have undertaken a RR study on microperoxidase-8 (MP8), a heme *c*-containing octapeptide. This product of digestion of horse cyt *c* with pepsin and trypsin obviously presents a heme with a chemical structure identical to that of its parent molecule (Harbury & Loach, 1960a,b). The octapeptide is indeed covalently bound to the heme and corresponds to the amino acid sequence 14–21 of cyt *c* with Cys 14 and 17 providing the two thioether linkages to heme (Figure 1). The presence of an imidazole side chain of a histidyl residue (His 18) immediately following the second of the thioether bridges is expected to provide an axial coordination to the heme group in neutral and alkaline aqueous solutions (Ehrenberg & Theorell, 1955; Tuppy & Paléus, 1955; Harbury & Loach, 1960a,b; Aron et al., 1986). Thus, the structure of MP8 retains the classical -Cys-X-Y-Cys-His- sequence of residues diagnostic of the heme-binding site of a large majority of *c*-type cytochromes (Margoliash & Schejter, 1966). Moreover, water soluble over a wide pH range, this heme compound is expected to offer the possibility of studying pentacoordinated complexes as well as six-coordinated complexes of different axial ligations if the solvent conditions were carefully controlled (Harbury & Loach, 1960b; Harbury et al., 1965). Finally, the use of cetyltrimethylammonium bromide, a cationic detergent, is expected to make accessible the deprotonation of the imidazole (ImH) group of His 18 in MP8 (Desbois & Lutz, 1985, 1992). We report in this paper the RR spectra of the monomeric form of reduced MP8 which is expected to simulate the heme structure and environment of cytochromes *c'*. A study on ferric and ferrous low-spin six-coordinated complexes of MP8 will be presented in a later paper.

EXPERIMENTAL PROCEDURES

Microperoxidase. Microperoxidase-8 from equine heart cytochrome *c* was purchased from Sigma and used without further purification. The reduced derivatives were prepared by addition of solid dithionite to MP8 solution under anaerobic conditions, i.e. under vacuum or by successive equilibrations with wet Ar gas atmosphere (Desbois et al., 1984a; Leondiadis et al., 1992). The effects of various aqueous conditions (pH, ionic strength) were investigated in order to monitor the aggregation and/or polymerization of MP8 (see Results and Discussion). To limit these phenomena, a detergent (cetyltrimethylammonium bromide (CTABr) (Sigma) or sodium dodecyl sulfate (NaDS) (BDH)) at a micelle-forming concentration of 1–2% (w/v)) or ethanol (EtOH) (Merck, spectroscopic grade) (50–70% (v/v)) was added to the solutions of MP8.

The buffers used were phosphate (50–100 mM, pH 7.0–7.5) and carbonate (50–100 mM, pH 10.0–10.5). For the very alkaline pH conditions (pH ≥ 12.0), NaOH or KOH (0.1–10 N) was added to the aqueous MP8 solutions.

Iron(II)–Protoporphyrin Derivatives. The 2-methylimidazole (2MeImH) and 2-methylimidazolate (2MeIm$^-$) complexes of Fe(II)–protoporphyrin were prepared in 2% aqueous CTABr solutions according to Mincey and Traylor (1979). Perdeuterated 2-MeImH (d_6–2MeImH) (isotopic enrichment 98.8%), D_2O (isotopic enrichment 99.8%), and NaOD (isotopic enrichment 98.5%, 9.8 N in D_2O) were purchased from the Bureau des Isotopes Stables of the Centre d'Etudes de Saclay.

In order to determine the resonance Raman spectra of mono(histidine) and mono(histidinate) derivatives of a reduced heme, various histidine derivatives complexed with ferroprotoporphyrin IX were prepared in 2% aqueous CTABr solutions using methods previously published (Desbois & Lutz, 1981, 1985). Hemin, L-histidine (His), L-histidine methyl ester (HisOMe), and N_α-(*tert*-butoxycarbonyl)-L-histidine (*N*-BocHis) were purchased from Sigma and used without further purification.

Spectroscopy. The Raman spectra were obtained using equipment described previously (Desbois et al., 1989). Samples were excited with 441.6-nm (Liconix He–Cd) and 413.1-nm (Coherent Innova Kr$^+$) lasers with radiant powers of 30–100 mW. Improvement in signal to noise ratio of the RR spectra was achieved by summations of 4–10 scans using a multichannel analyzer (Tracor Northern TN 1710). Under these conditions, the frequency precision is 0.5–2 cm^{-1} depending on the band intensity. In these experiments, the HP8 concentration was 0.1–1.0 mM. The spectrophotometric measurements were done using Cary 118C or Beckman DU7 recording spectrophotometers.

RESULTS AND DISCUSSION

Absorption Spectroscopy. The electronic absorption spectra of MP8(II) at pH 7.5–12.0 in aqueous buffered solutions exhibit a Soret band at 414 nm with a shoulder at ~430 nm. In the visible region, bands are observed at ~521, ~549, and ~570 nm (spectra not shown). These features characterize a major contribution of a low-spin (LS) heme complex. As in numerous heme compound systems, the absorption spectrum of MP8(II) is pH-, ionic strength-, and MP8 concentration-dependent. These sensitivities are related to heme aggregation (Harbury & Loach, 1960a,b; Urry & Pettigrew, 1967; Aron et al., 1986) and possibly to peptide polymerization.

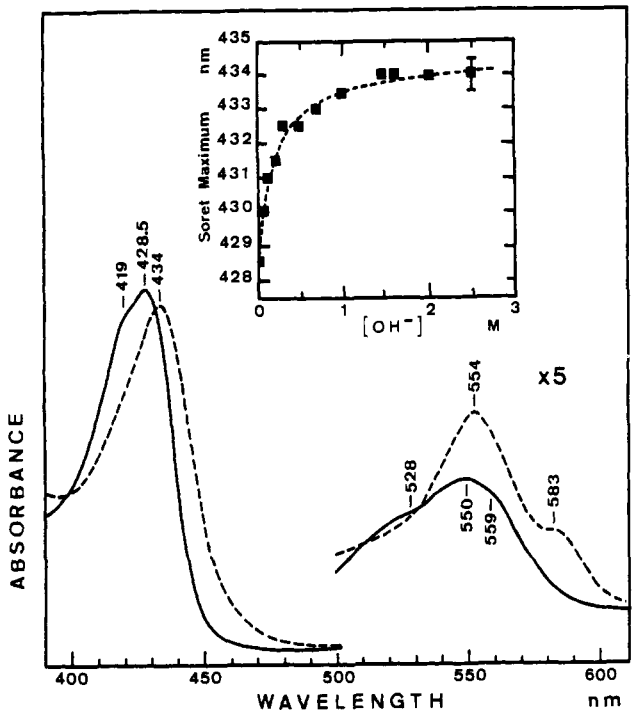

FIGURE 2: Electronic absorption spectra of MP8(II) in 2% aqueous CTABr solution at pH = 7.5 (50 mM phosphate buffer) (—) and in 2.5 M NaOH (- - -). Inset: Hydroxide concentration dependence of the Soret maximum of MP8(II) in 2% aqueous CTABr solutions. The theoretical curve is drawn according to a one-step proton ionization of MP8(II) with a pK_a value of 13.3 ($c_{1/2}(OH^-)$ = 0.2 M).

These phenomena are expected to be restricted by the addition of a dispersing agent (a detergent or a water-miscible solvent) in the aqueous solutions of MP8(II). Figure 2 shows the absorption spectrum of dithionite-reduced MP8 in 2% aqueous CTABr solution at pH 7.5. It exhibits a Soret band at 428.5 nm and a shoulder on its short-wavelength side at ca. 419 nm. The α and β bands are detected at 559 and 550 nm, respectively with a shoulder at 528 nm (Figure 2). These spectral characteristics essentially correspond to a five-coordinated high-spin (HS) complex. Histidinate (His^-) and imidazolate (Im^-) complexes of ferroprotoporphyrin IX (Fe(II)–ProtoP) have been previously generated in aqueous CTABr solutions at very alkaline pH (Desbois & Lutz, 1985, 1992). Under these conditions, the spectrum of MP8(II) presents red shifts of the absorption bands with α, β, and Soret bands at 583, 553, and 434 nm, respectively (Figure 2). Titrations performed at fixed wavelengths or based on the observation of the apparent Soret maximum show that this spectral transition is in one step and corresponds to either the binding of one hydroxide anion or the neutralization of one proton with an apparent pK_a value of 13.3 (Figure 2, inset). Since (i) the red shift in the positions of the Soret and visible absorption bands as well as the appearance of a resolved band at 583 nm in the spectrum of the alkaline form of MP8(II) are optical features associated with a deprotonated axial imidazole (Mincey & Traylor, 1979) and (ii) the pK_a value for the deprotonation of the axial ligand of Fe(II)–ProtoP-(2MeImH) in a 2% aqueous CTABr solution is 13.6 (A. Desbois, unpublished data), we favor the interpretation of the His deprotonation of MP8(II) in aqueous alkaline CTABr solution.

The absorption spectra of MP8(II) in 2% aqueous NaDS or in 50% aqueous EtOH, at pH 7.5, present major contributions of a HS signal. The Soret band is indeed observed at 425 and 432 nm, in aqueous NaDS and aqueous EtOH,

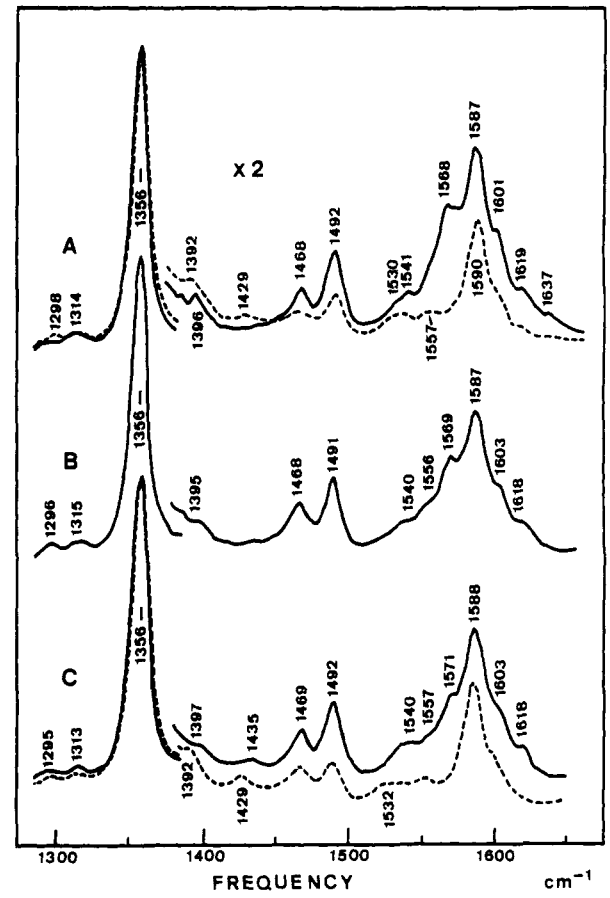

FIGURE 3: High-frequency regions (1300–1650 cm^{-1}) of resonance Raman spectra of MP8(II) in water: (A) pH = 7.5 (50 mM phosphate); (B) NaOH 0.1 M; (C) NaOH 1 M. Excitations: 441.6 (—) and 413.1 (- - -) nm.

respectively (spectra not shown). However, this spectral region also clearly exhibits a more or less intense shoulder or even a weak band at ca. 414 nm, indicating low but significant levels of a polymeric LS form of MP8(II).

In conclusion, the Soret band maximum of the HS form of MP8(II) varies between 425 and 434 nm depending on the solvent conditions. Similar absorption spectra were obtained for the neutral form of various ferrous cyt c' which exhibits a Soret band in the 423–436-nm region (Bartsch, 1978; Yoshimura et al., 1985).

High-Frequency Regions of Resonance Raman Spectra. The frequencies of the skeletal stretching modes of hemes and hemoproteins, located in the 1300–1650-cm^{-1} regions of resonance Raman (RR) spectra, are sensitive to the ligation and spin state of the metal atom (Spiro, 1985; Kitagawa & Ozaki, 1987). Figures 3 and 4 display these spectral regions of MP8(II) in various aqueous solvents. The RR spectra of MP8(II) in water are consistent with a mixture of HS and LS species, since doublets are clearly seen for the spin state sensitive modes, i.e. at ~1468 and ~1492 cm^{-1} (ν_3), ~1569 and ~1587 cm^{-1} (ν_2), and ~1602 and ~1618 cm^{-1} (ν_{10}) (Figure 3). The first set of frequencies (1468, 1569, and 1602 cm^{-1}) characterizes a HS five-coordinated heme while the second series (1492, 1587, and 1618 cm^{-1}) corresponds to a LS six-coordinated heme. The major contribution of this latter form is consistent with intermolecular bonding of MP8 when dissolved in water (Harbury & Loach, 1960a,b; Aron et al., 1986). When MP8(II) is dispersed in neutral aqueous solutions containing a detergent or EtOH, the RR spectra are modified with major contributions of bands at ~1469, ~1571, and ~1605 cm^{-1} which indicate a conversion to a five-

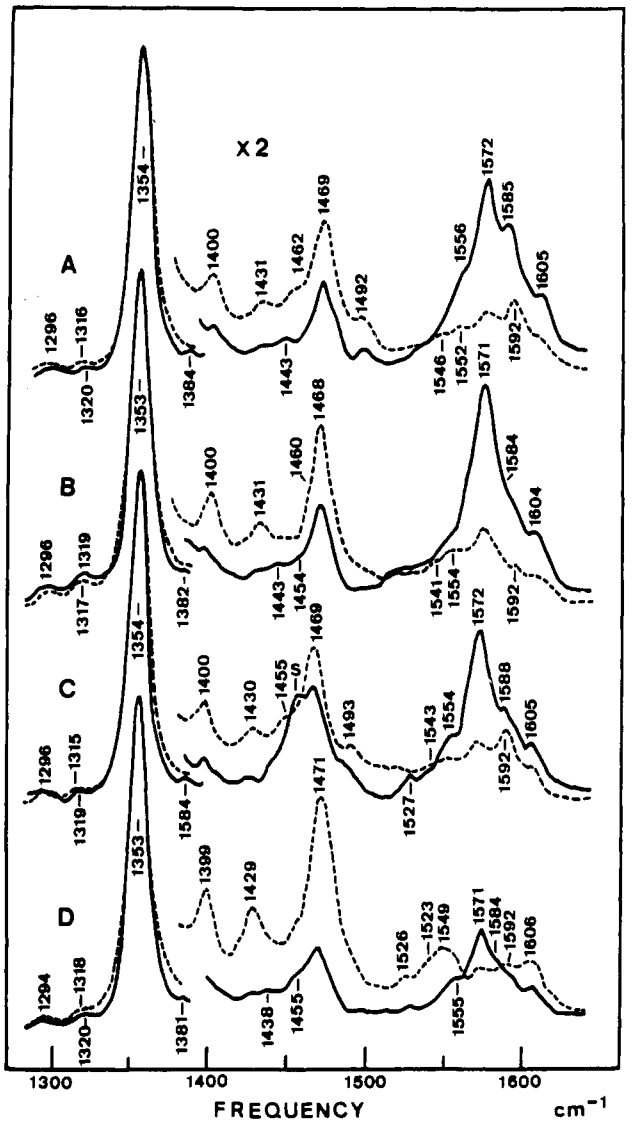

FIGURE 4: High-frequency regions (1300–1650 cm^{-1}) of resonance Raman spectra of MP8(II) in (A) 2% aqueous NaDS solution at pH = 7.5 (50 mM phosphate); (B) 2% aqueous CTABr solution at pH = 7.5 (50 mM phosphate); (C) 50% aqueous ethanol solution at pH = 7.5 (50 mM phosphate), S corresponds to a solvent band; (D) 2% aqueous CTABr solution in 2.5 M NaOH. Excitations: 441.6 (—) and 413.1 (- - -) nm.

coordinated HS form (Figure 4). However, the presence of a band at ~1492 cm^{-1} shows that there still persists a small contribution of a six-coordinated LS form of MP8(II) in the presence of NaDS or EtOH (Figure 4, spectra A and C). These observations are fully consistent with the above-presented absorption data.

On the other hand, the deprotonation of MP8(II) in 2% aqueous CTABr solution provokes a decrease in intensity of RR bands in the 1450–1650-cm^{-1} region (Figure 4, spectra B and D). Moreover, significant shifts in frequency of the ν_3 (1468 → 1471 cm^{-1}) and ν_{10} (1604 → 1606 cm^{-1}) modes are clearly detected. No significant contribution of a LS signal is found using either the 441.6- or 413.1-nm excitation.

Peripheral Effects on the Porphyrin Modes. The high-frequency regions of RR spectra of metalloporphyrins contain several bands that are correlated to the porphyrin core size (Choi et al., 1982; Parthasarathi et al., 1987). On the other hand, the frequencies of some of these bands are strongly sensitive to the nature of peripheral porphyrin substituents (Choi et al., 1982, 1983; Desbois et al., 1984a). In a series

Table I: High-Frequency Raman Modes (in cm^{-1}) of Monomeric MP8(II)

	MP8(II)					
	CTABr		NaDS	EtOH	cyt *c*′(II)[a]	
mode[b]	pH 7.5	alk pH	pH 7.5	pH 7.5	pH 6.9–7.3	assignment[b]
$\nu_5 + \nu_9$	1296	1295	1298	1296		
ν_{21}	1318	1319	1318	1316	1319–1324	$\nu(C_\alpha N) + \delta(C_\beta C)$
ν_4	1353	1355	1352	1352	1352–1355	$\nu(C_\alpha C_\beta) + \nu(C_\alpha N)$
ν_{29}	1393	1395	1394	1398		$\nu(C_\alpha C_\beta)$
ν_{20}	1401	1400	1401	1401	1401–1403	$\nu(C_\alpha C_\beta)$
	1432	1429	1431	1430		
ν_{28}	1456	1454	1460	1454		$\nu(C_\alpha C_m)$
ν_3	1468	1470	1469	1469	1469–1475	$\nu(C_\alpha C_m) + \nu(C_\beta C_\beta)$
ν_{38}	1532	1533		1530		$\nu(C_\beta C_\beta)$
ν_{19}	1545	1549	1543	1545		$\nu(C_\alpha C_m)$
ν_{11}	1555	1557	1554	1555	1548–1551	$\nu(C_\beta C_\beta)$
ν_2	1570	1572	1572	1572		$\nu(C_\beta C_\beta)$
ν_{37}	1585	1585	1586	1586	1575–1583	$\nu(C_\alpha C_m)$
ν_{10}	1603	1606	1604	1605	1604–1609	$\nu(C_\alpha C_m)$

[a] RR data for the neutral form of cyt *c*′ from *Alcaligenes sp. N.C.I.B. 11015*, *Rhodospirillum rubrum*, *Rhodopseudomonas palustris*, and *Chromatium vinosum* (Strekas & Spiro, 1974; Kitagawa et al., 1977; Yoshimura et al., 1985; Hobbs et al., 1990). [b] Mode numbering and assignment from Li et al. (1990b).

Table II: Frequencies (in cm^{-1}) of the ν_2, ν_{11}, and ν_{29} Porphyrin Modes of High-Spin, Five-Coordinated Fe(II)–Heme IX Complexes[a]

	porphyrin mode		
derivative	ν_2	ν_{11}	ν_{29}
Fe(II)–MesoP(2MeImH)	1583	1558	1400
Fe(II)–HematoP(2MeImH)	1579	1557	1395
Fe(II)–DeuteroP(2MeImH)	1573	1556	1395
MP8(II)	1572	1555	1394
Fe(II)–ProtoP(2MeImH)	1562	1549	1392

[a] RR data from Spiro and Burke (1976) and Desbois et al. (1984a).

of HS five-coordinated ferroheme IX compounds, the ν_2, ν_{11}, and ν_{29} modes have appeared to be the most sensitive to the inductive effects of the 2- and 4-pyrrole substituents (Desbois et al., 1984a). These effects apparently perturb the frequency of modes primarily associated with $C_\beta C_\beta$ stretching vibrations (Abe et al., 1978; Li et al., 1990a,b). Table II shows that the thioether linkages of MP8 ($CH(CH_3)$–S–CH_2 substituents) influence the porphyrin modes in a way similar to that of the 2- and 4-protons of deuteroporphyrin (Desbois et al., 1984a). In fact, this indicates that the positive inductive effect of the >CH–CH_3 group practically cancels out the negative inductive effect of the thiomethylene group (S–CH_2). From these RR data, MesoP and OEP are therefore poor models for a simulation of peripheral electronic effects of heme *c*, the most relevant porphyrin system for this modeling appearing to be deuteroporphyrin (Table II).

On the other hand, in the determination of the core size of *c*-type heme, the parameters *A* and *K* of the ν_2 and ν_{11} modes have to be modified in order to take into account the peripheral changes from vinyl groups in the *b*-type hemes to thioether groups in the *c*-type hemes. With reference to the RR data obtained for the HS five-coordinated forms of MP8(II) (Figure 4) and the imidazole complex of ferric MP8 (LS six-coordinated) (data not shown), the ν_2 and ν_{11} correlations obtained from the metallo-protoP derivatives (Parthasarathi et al., 1987) seem to be roughly shifted without important changes in slope (K = 295.4 and 381.8 $cm^{-1}/Å$, A = 7.36 and 6.09 Å for ν_2 and ν_{11}, respectively.

Low-Frequency Regions of Resonance Raman Spectra. A mode involving the iron–axial ligand stretching has been identified in the 210–240-cm^{-1} regions of five-coordinated HS ferrous hemoproteins and model compounds (Kitagawa

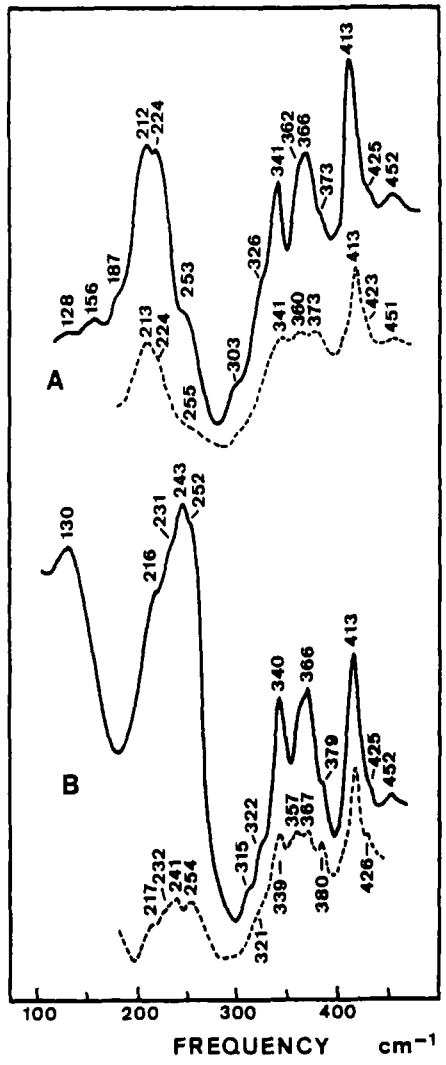

FIGURE 5: Low-frequency regions (100–460 cm^{-1}) of resonance Raman spectra of MP8(II) in 2% aqueous CTABr solution: at pH = 7.5 (50 mM phosphate) (spectrum A) and in 2.5 M NaOH (spectrum B). Excitations: 441.6 (—) and 413.1 (- - -) nm.

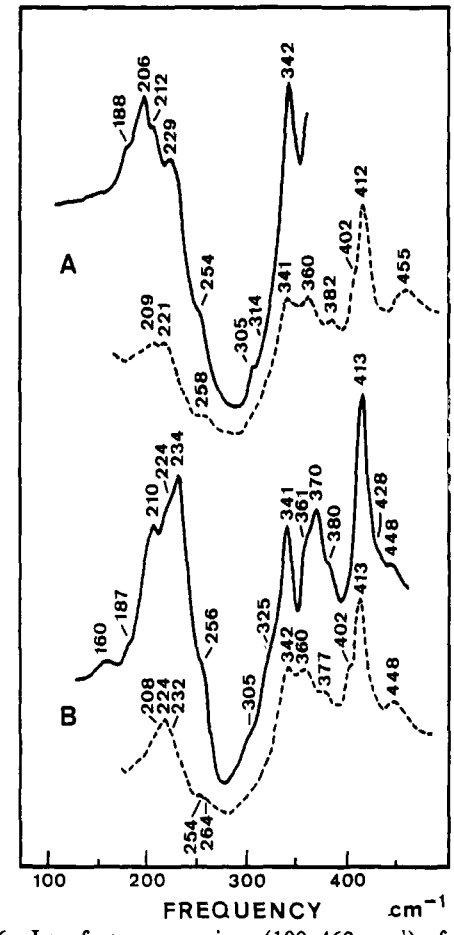

FIGURE 6: Low-frequency regions (100–460 cm^{-1}) of resonance Raman spectra of MP8(II) in (A) 2% aqueous NaDS solution at pH = 7.5 (50 mM phosphate); (B) 50% aqueous ethanol solution at pH = 7.5 (50 mM phosphate). Excitations: 441.6 (—) and 413.1 (- - -) nm.

et al., 1979; Kincaid et al., 1979; Nagai et al., 1980). However, other experimental or theoretical data indicate that this axial mode is significantly coupled with an internal mode of the imidazole ring (Argade et al., 1984; Wells et al., 1991) as well as with a porphyrin mode (Desbois et al., 1981b; Stavrov, 1993). Although the extent of these couplings likely depends on the conformation of the FeN_4(pyrrole)–imidazole grouping, the frequency of the 210–240-cm^{-1} band nonetheless remains an indicator of the strength of heme–ligand interaction in five-coordinated HS ferrous hemes and hemoproteins.

In the absence of isotopically labeled derivatives, vibrational assignments of the 200–260-cm^{-1} bands of MP8(II) can be made by comparing their spectra (Figures 5 and 6) with those of 2MeImH and 2MeIm$^-$ complexes of Fe(II)–ProtoP (Figure 7), for which assignments have been proposed on the basis of isotopic substitutions (Hori & Kitagawa, 1980; Teraoka & Kitagawa, 1981) (Figure 7). The 252–256-cm^{-1} shoulders in the spectra of MP8(II) have their homologous bands at 254–258 cm^{-1} in the spectra of five-coordinated Fe(II)–ProtoP derivatives (Kincaid et al., 1979; Nagai et al., 1980; Desbois & Lutz, 1981; Desbois et al., 1984a) (Figures 5–7). These bands which are shifted to 263–268 cm^{-1} in the RR spectra of six-coordinated Fe(II)–ProtoP and MP8(II) derivatives (Desbois & Lutz, 1992; spectra not shown) are assigned to ν_9 (Li et al., 1990b) (Table III). On the other hand, the 441.6-nm excited spectra of Fe(II)–ProtoP complexed to an imidazole ring exhibit only one band in the 190–250-cm^{-1} regions (Hori & Kitagawa, 1980; Desbois & Lutz, 1981; Teraoka & Kitagawa, 1981) (Figure 7). Using ligand perdeuterations, this band has been assigned to a FeN(ligand)-involving mode (Teraoka & Kitagawa, 1981). Figures 5 and 6 show different sets of overlapping bands in these regions that could correspond to a multiplicity of ν(FeHis) modes in MP8(II). However, we cannot exclude that the change in the peripheral composition from heme *b* to heme *c* makes active deformation modes of the porphyrin substituents, in particular those involving the thioether bridges, as well as porphyrin modes. To support this suggestion, Figures 5 and 7 represent the RR spectra of the limiting forms of alkaline titrations of MP8(II) and Fe(II)–protoP(2MeImH) in aqueous CTABr solutions. The deprotonation of Fe(II)–ProtoP(2MeImH) produces a 21-cm^{-1} upshift of the ν(Fe–ligand) mode (Figure 7). For MP8(II) excited at 441.6 nm, only the 224-cm^{-1} band is apparently shifted to a similar amount (19 cm^{-1}) upon histidine deprotonation (Figure 5). On the basis of this sensitivity to the ionization state of the ligand, the 224- and 243-cm^{-1} bands of MP8(II) in aqueous CTABr detergent (spectra A and B, respectively, Figure 5) are assigned to ν-(FeHis)-involving modes. Conversely, the weak sensitivity in frequency of the 212–216-cm^{-1} band makes unprobable its involvement in an axial mode (Figure 5). Moreover, bands of moderate intensity are also detected at 212–220 cm^{-1} in the RR spectra of ligated forms of MP8(II) (not shown).

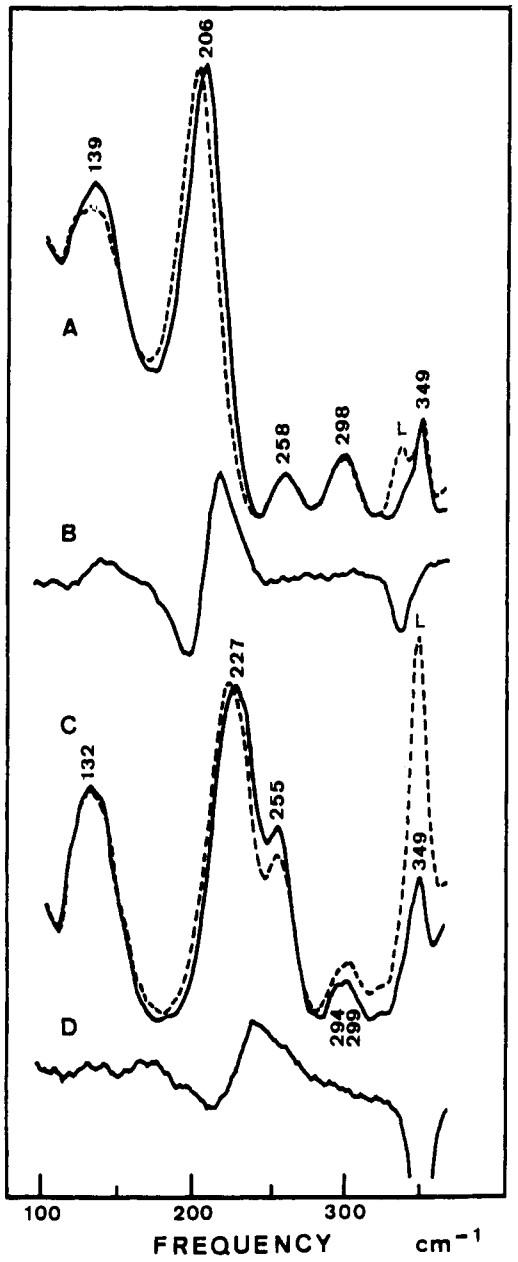

FIGURE 7: (A) Effect of ligand perdeuteration on the 100–360-cm^{-1} regions of RR spectra of Fe(II)–ProtoP(2MeImH) in 2% aqueous (H_2O or D_2O) CTABr solutions: excitation 441.6 nm; summations of 14 scans; 2MeImH concentrations (h_6- or d_6-2MeImH) 60 mM. (B) Difference of the preceding RR spectra: the S shaped band corresponds to a 4.8 (±0.2) cm^{-1} shift of the 206-cm^{-1} band (Rousseau, 1981). (C) Effect of ligand perdeuteration on the 100–360-cm^{-1} regions of RR spectra of Fe(II)–protoP(2MeIm$^-$) in 2% aqueous (H_2O or D_2O) CTABr solutions: excitation 441.6 nm; summations of 17 scans; ligand concentrations 100 mM; final hydroxide concentrations were adjusted at 1.5 M by addition of aqueous NaOH or NaOD. (D) Difference of RR spectra in C: the S shaped band corresponds to a 3.2 (±0.3) cm^{-1} shift of the 227-cm^{-1} band. The band marked with L in spectra A and C is due to a free ligand band.

The ν(FeN(ligand)) mode of Fe(II)–ProtoP(2MeImH) is sensitive to the H-bonding capability of the solvent. Its frequency is indeed shifted from 200 cm^{-1} in an organic solvent to 210 cm^{-1} in water (Teraoka & Kitagawa, 1981). Figure 6 displays the RR spectra of MP8(II) in solvents of different polarities. Besides common bands recognizable at 187–188, 210–212, and 254–256 and already seen in the spectra of Figure 5, two specific bands are observed at 206 and 229 for MP8(II) in aqueous NaDS. In the case of MP8(II) in a more polar solvent (aqueous EtOH), the 441.6-nm excitation shows

Table III: Low-Frequency Raman Modes (in cm^{-1}) of Monomeric MP8(II)

	MP8(II)					
	CTABr		NaDS	EtOH	cyt c'(II)[a]	
mode[b]	pH 7.5	alk pH	pH 7.5	pH 7.5	pH 7.0	assignment[b]
	128	130				
	156			160		
	187		188	187		
	212	216	212	210		
	224	243	206	234	232	ν(FeHis)
			229			
ν_9	254	253	254	255		
ν_{17}	303	315	305	305		$\delta(C_\beta C)$
	326	322	314	325		
ν_8	341	340	342	341	347	
	361	357	360	361		Pyr tilt
$2\nu_{35}$	366	366	366	370		
	373	379	382	376		Pyr tilt
$\nu_{34} + \nu_{35}$	413	413	412	413		
	425	425		428		
	452	452	455	448		$\delta(C_aC_m)$
	543	543		545		
	634	637		636		
	664	655		662		
ν_7	688	686		688		$\delta(C_aC_mC_a) + \nu(C_aN)$
	722	722		723		

[a] RR data for cyt c' from *Chromatium vinosum* (Hobbs et al., 1990). [b] Mode numbering and assignment from Li et al. (1990b).

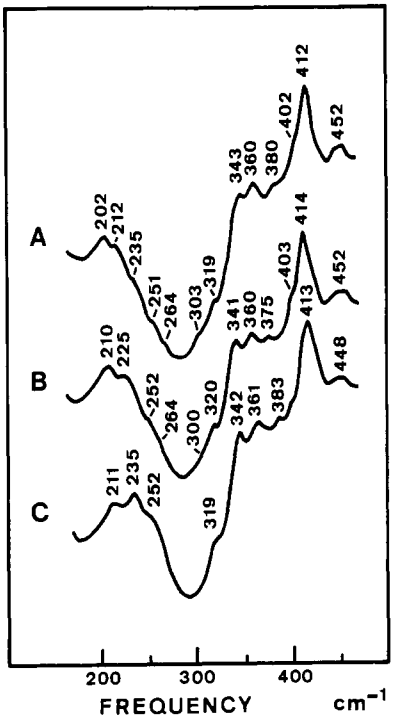

FIGURE 8: Low-frequency regions (160–460 cm^{-1}) of resonance Raman spectra of MP8(II) in water: (A) pH = 7.5 (50 mM phosphate buffer); (B) NaOH 0.1 M; (C) NaOH 1M. Excitation: 441.6 nm.

two specific bands at 224 and especially 234 cm^{-1} (Figure 6). These sensitivities to the solvent polarity which are similar to that of the ν(Fe2MeImH) mode of Fe(II)–ProtoP(2MeImH) suggest a ν(FeHis) involvement for the bands at 206 and 229 cm^{-1} (aqueous NaDS) and 224 and 234 cm^{-1} (aqueous EtOH).

Although MP8(II) presents a strong trend to form intermolecularly bound compounds in water, a significant contribution of five-coordinated HS monomeric MP8(II) remains observable in the high-frequency RR spectra (Figure 3). In the low-frequency regions, the 200–240-cm^{-1} regions exhibit a sensitivity to pH (Figure 8). Common bands are again observed at ~211 and ~252 cm^{-1}. The remainder, i.e. the

202, 235 (pH 7.5), 225 (pH 13.0), and 235 (pH 14.0) cm^{-1} bands are assigned to ν(FeHis)-involving modes. These frequencies are close to those detected in the presence of NaDS (206 and 229 cm^{-1}), CTABr (224 cm^{-1}), or EtOH (234 cm^{-1}) at pH 7.5 (Figures 5 and 6).

One may point out that the frequencies of RR bands located in the 300–330-cm^{-1} regions of RR spectra of MP8(II) also differ significantly with the solvent composition (Figures 5 and 6). These spectral alterations indicate modifications in the heme environment (Desbois et al., 1984b).

MP8(II) as a Model for Reduced cyt c'. The cytochromes *c'* form an anomalous class of *c*-type cytochrome occurring in photosynthetic, denitrifying, and nitrogen-fixing bacteria. High-spin in the reduced state (Meyer & Kamen, 1982), the fifth coordination site of the ferric heme is occupied by the N_1 atom of a histidylimidazole ring while the sixth coordination is vacant (Weber et al., 1981). Both absorption and high-frequency RR spectra show that the monomeric form of MP8-(II) is five-coordinated HS from pH 7.0 to 14.5 (Figures 2 and 4). The low-frequency RR spectra further demonstrate that the imidazole ring of His coordinates the heme intramolecularly, as earlier assumed (Tuppy & Paléus, 1955; Ehrenberg & Theorell, 1955). Considering both the axial ligation and the peripheral composition of heme, MP8(II), therefore, constitutes a relevant model compound for reduced *c'*-type cytochromes. Different cytochromes *c'* have been investigated using RR spectroscopy (Strekas & Spiro, 1974; Kitagawa et al., 1977; Yoshimura et al., 1985; Hobbs et al., 1990). Table I compares the frequencies of skeletal porphyrin modes of MP8(II) and cyt *c'*(II) from various sources and indicates that some porphyrin modes (ν_3, ν_{11}, ν_{37}, and ν_{10}) of hemoproteins exhibit significant frequency shifts with respect to the corresponding frequencies obtained for the hemopeptide. These deviations could be related to out of plane heme deformations (ruffling, doming) introduced by various protein strains.

The RR data concerning the low- and medium-frequency modes of cyt *c'* are still scarce. A recent investigation has however detected two bands at 232 and 347 cm^{-1} in the spectra of cyt *c'*(II) from *Chromatium vinosum* (Hobbs et al., 1990). The former band has been proposed to correspond to the ν-(FeHis)-involving mode (see below).

Octapeptide Structure. In horse cyt *c*, residues 14–17 form a 3_{10} helix segment that positions the two thioether attachment points while the 17–21 sequence adopts a random-coiled structure (Bushnell et al., 1990) (Figure 9). The imidazole-(His 18)–heme geometry is however relatively fixed with the imidazole plane bisecting the iron–pyrrole bonds, making impossible the rotation of the iron–imidazole bond. As far as the MP8 peptide is concerned, its structure is unknown but likely more relaxed than in cyt *c*. A conformational rigidity is expected for the residues 14–18 with the maintenance of the two thioether bridges and the His coordination to the heme iron. Moreover, a loop is conserved for the 14–17 sequence, since it is determined during the cyt *c* biosynthesis and not disrupted after proteolysis. In addition, a space-filling model indicates the same structure for the heme–histidylimidazole coordination for cyt *c* and MP8 [M. D. Frechter, quoted in Smith and Mc Lendon (1981)]. However, The N_1 proton of His 18 in cyt *c* is H-bonded with Pro 30, which is absent in MP8. Therefore, the C-terminal end of MP8 (sequence 19–21) appears to be flexible and could interact with the imidazole group of His, according different geometries.

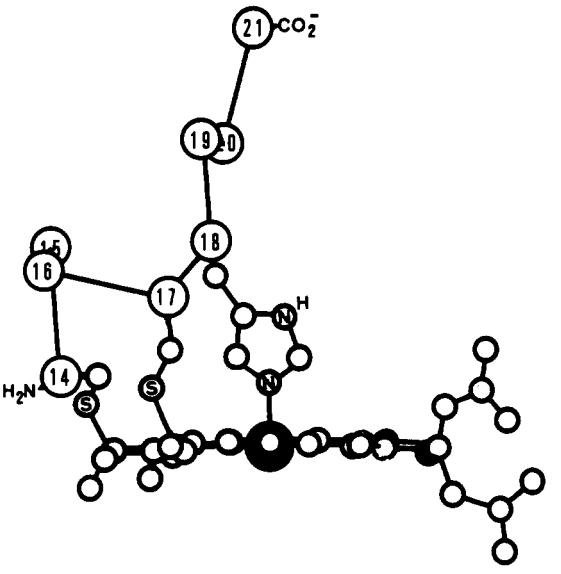

Cys-Ala-Gln-Cys-His-Thr-Val-Glu
14 15 16 17 18 19 20 21

FIGURE 9: Schematic representation of the MP8 structure in cytochrome *c*. This drawing is adapted from the X-ray structure of horse heart cyt *c* (Bushnell et al., 1990).

Different approaches indicate that the octapeptide of MP8 could adopt a helical secondary structure (Erhenberg & Theorell, 1955; Jehanli et al., 1976; Wilson et al., 1977). Nevertheless, various spectroscopic data show that small oligopeptides can form helices, sheets, or coils (Mattice, 1989), the stabilization of one of these structures depending on the solvent conditions (Dill, 1990), i.e. pH, ionic strength, and the presence of a detergent (Sarkar & Doty, 1966; Maeda et al., 1988) or of a cosolvent (Fronticelli & Gold, 1976; Iyer & Acharaya, 1986). Therefore, the C-terminal part of the octapeptide could undergo conformational changes when exposed to various solvent conditions. In particular, the electrostatic interactions between a micelle of detergent (cationic and anionic for CTABr and NaDS, respectively) and the terminal Glu residue of MP8 (anionic by the presence of two carboxylate groups) certainly play a crucial role in the peptide structuration (Figure 9). Thus, one may expect that the solvent dependence of the ν(FeHis)-involving mode of MP8(II) represents different orientations of the C-terminal end of the octapeptide backbone and their amino acid side chains, which could primarily alter the H-bonding interaction between the (imidazole)N_1-H group of His 18 and the peptide or the solvent. Additional experiments to explore the peptide conformation of MP8 in different solvents will be useful.

H-Bonding and Deprotonation of the Coordinated Histidine. The deprotonation of 2MeImH bound to Fe(II)-OEP in dimethylformamide shifts the frequency of the ν(Fe–ligand) mode by ca. 26 cm^{-1}, from 208–212 to 233–239 cm^{-1} (Stein et al., 1980; Teraoka & Kitagawa, 1981). For Fe(II)–ProtoP-(2MeImH) and Fe(II)–ProtoP(2MeIm$^-$) in 2% aqueous CTABr solutions, the frequency shift is only 21 cm^{-1}, from 206 to 227 cm^{-1} (Figure 7). However, all these frequencies are influenced by H-bonding between bound and free ligand (Stein et al., 1980), since the imidazole groups with no ring substituent in positions 1 and 3 are both proton donors and proton acceptors (Del Bene & Cohen, 1978) and the ligand concentrations used in these experiments largely favor the

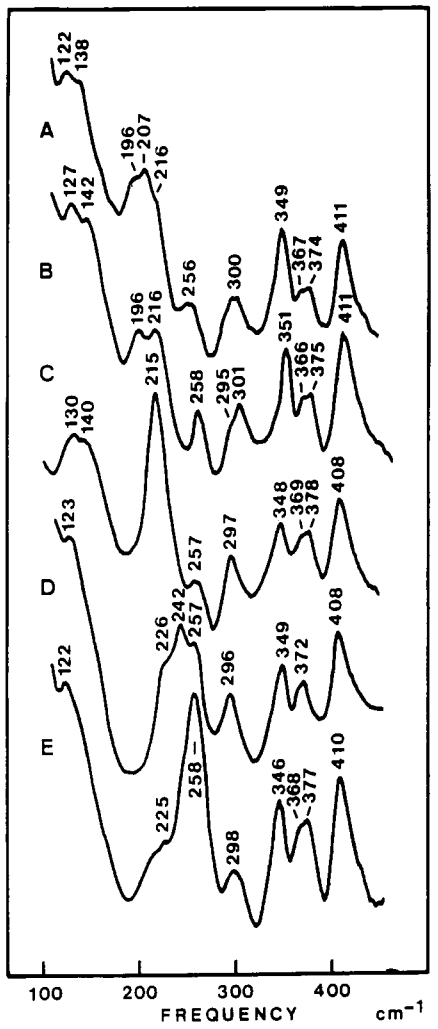

FIGURE 10: Low-frequency regions (100–450 cm^{-1}) of various mono(histidine) derivatives of Fe(II)ProtoP in 2% aqueous CTABr solutions: excitation wavelength, 441.6 nm; (A) His (200 mM) pH 8.0; (B) HisOMe (25 mM) pH 8.6; (C) *N*-BocHis (4 mM) pH 7.2; (D) *N*-BocHis (4 mM) NaOH 1.4 N; (E) His (200 mM) NaOH 1.5 N. Accumulation of 6–8 scans.

ligand interactions (Stein et al., 1980; Teraoka & Kitagawa, 1981). On the other hand, the steric contribution of the 2-methyl group of 2MeImH and $2MeIm^-$ on the frequency of the ν(Fe–ligand) modes is currently unknown.

In order to explore the frequency variation of the ν(Fe–ligand) mode of His and His^- compounds of a ferroporphyrin, we have obtained the RR spectra of various mono(His) and mono(His^-) complexes of Fe(II)–ProtoP using previously published methods (Desbois & Lutz, 1981, 1985). The insensitivity of the ν(Fe2MeImH)-involving mode to the nature of heme substituents in positions 2 and 4 on the pyrrole rings of Fe(II)–porphyrin(2MeImH) complexes indeed allows the direct comparison of ν(FeHis) modes of *b*- and *c*-type hemes (Desbois et al., 1984a). At variance with the 190–250-cm^{-1} regions of RR spectra of 2MeImH and $2MeIm^-$ complexes of Fe(II)–ProtoP which show a single band for the ν(Fe–ligand) mode (Figure 7), those of His, HisOMe, and *N*-BocHis complexes of Fe(II)–ProtoP at pH 7–9 exhibit from one to three bands (Figure 10). Recalling that the blue-excited RR spectra of various mono(imidazole) complexes of Fe(II)–ProtoP do not present any porphyrin or peripheral mode in this spectral region (Teraoka & Kitagawa, 1981) (Figure 7), all of these bands are therefore assigned to ν(FeHis)-involving modes. The fact that the number, frequency, and intensity of these bands are dependent both on the pH value and the

Table IV: Frequencies (in cm^{-1}) of the ν(FeHis)-Involving Modes of Reduced MP8, Heme Compounds, and Hemoproteins[a]

derivative	ν(FeHis)	protonation and H-bonding states of the heme-bound His
Fe–ProtoP(HisOMe) (CTABr, pH 7.5)	196	$(His)N_1H$
MP8 (H_2O, pH 7.5)	202	$(His)N_1H$ or
MP8 (NaDS, pH 7.5)	206	$(His)N_1H\cdots OH_2$
Mb *Aplysia*	210	
human Hb	215	
Mb sperm whale	220	
Mb horse	222	$(His)N_1H\cdots OC$(peptide)
Hb *Glycera*	222	
Lb soybean	224	
MP8 (CTABr, pH 7.5)	224	
MP8 (NaDS, pH 7.5)	229	
cyt *c'* (pH 7)	232	$(His)N_1^-\cdots HN(Arg^+)$
MP8 (EtOH, pH 7.5)	234	$(His)N_1H\cdots {}^-O_2C$(Glu)
HRPC (pH 8)	243	$(His)N_1^-\cdots H_2N$(Gln or Lys)
MP8 (CTABr, KOH)	243	$(His)N_1^-\cdots HN$(peptide) or $(His)N_1^-\cdots HO$(Thr)
TP 7 (pH 7–8)	246	$(His)N_1^-\cdots HN$(Arg) or $(His)N_1^-\cdots H_2N$(Gln)
CcP (neutral form)	248	$(His)N_1^-\cdots HO_2C$(Asp)
TP 1 (pH 7–8)	251	$(His)N_1^-\cdots HO_2C$(Asp) or $(His)N_1^-\cdots H_2N$(Asn)
Fe–ProtoP(His^-) (CTABr, KOH)	258	$(His)N_1^-$

[a] RR data from Teraoka et al. (1983), Desbois et al. (1984b), Desbois and Lutz (1985), Dasgupta et al. (1989), Hobbs et al. (1990), and this work. X-ray crystallographic data from Takano (1977), Arutyunyan (1981), Fermi et al. (1984), Finzel et al. (1984), Arents and Love (1989), Bolognesi et al. (1989), and Evans and Brayer (1990).

presence of a blocking reagent on the ionizable groups of His (Figure 10) clearly indicates that internal H-bonds could be engaged between the carboxylic or the amine group of the imidazole side chain and the (imidazole)N_1 proton of bound His, as is the case for free His (Roberts et al., 1982). A more complete description of these new spectroscopic data as well as a detailed discussion on the possible structures of mono(His) complexes of Fe(II)ProtoP will be the subject of a separate publication. On the other hand, the alkaline titration of Fe(II)–ProtoP(His) in an aqueous CTABr solution produces a disappearance of the 196–215-cm^{-1} bands and the predominence of a band at 258 cm^{-1} (Desbois & Lutz, 1985; Figure 10). By analogy with the spectral transition observed for the ligand ionization of Fe(II)–ProtoP(2MeImH) (Figure 7), the 258-cm^{-1} band of the alkaline form of Fe(II)–ProtoP(His) is assigned to a ν($FeHis^-$) mode.

The lowest frequency observed for a HS five-coordinated complex of Fe(II)–ProtoP with a His derivative has been detected at 196 cm^{-1} (Figure 10) (Table IV). We infer that this frequency corresponds to a histidylimidazole ring bound to the heme iron with no H-bonding interaction at its N_1–H group. A H-bond at this site is expected to increase the electronegativity of the imidazole group, the ligand field strength, and therefore the frequency of the ν(FeHis)-involving mode. On the contrary, the highest frequency for this mode is observed at 258 cm^{-1} for the mono(His^-) complex to Fe(II)–ProtoP (Desbois & Lutz, 1985; Figure 10). We propose that this frequency corresponds to an isolated His^- anion bound to heme. In this opposite case, any H-bonding interaction at the N_1 atom of the imidazolate ring is expected to decrease its electronegativity, its ligand field strength, and therefore the ν($FeHis^-$) frequency. Thus, the 62-cm^{-1} frequency shift (196–258 cm^{-1}) of the ν(FeHis)-involving mode of HS five-coordinated ferroheme–His compounds seems to be primarily

determined by the H-bonding and deprotonation states of the histidylimidazole ring involved in the axial bond (Stein et al., 1980; Teraoka & Kitagawa, 1981; Desbois & Lutz, 1985), strain and/or tilt of the Fe–His linkage appearing to be of secondary importance since these bond deformations decrease this frequency by 4–20 cm^{-1} (Nagai et al., 1980; Desbois et al., 1981a; Chaudhury et al., 1992). Taking into account that bound His and His^- are a proton donor and a proton acceptor, respectively, two overlapping scales of opposite direction may thus be drawn: A first scale (the "histidine" scale), beginning at 196 cm^{-1}, with increasing frequencies corresponding to increasing H-bonding strengths between the heme-bound His and a proton acceptor [(His)$N_1H\cdots X^{\delta-}$] and a second scale (the "histidinate" scale), starting at 258 cm^{-1}, with decreasing frequencies corresponding to increasing H-bonding strengths between a bound His^- and a proton donor [(His)$N_1^-\cdots HY$]. An overlap of these two scales obviously lies in a 230–240-cm^{-1} range where ambiguities may exist about the ionization state of His.

The maximal shift of the ν(FeHis) mode of MP8(II) is 41 cm^{-1} (202–243 cm^{-1}) (Table III). Considering that obtained for mono(His) and mono(His^-) compounds of Fe(II)–ProtoP (258 – 196 = 62 cm^{-1}), we can conclude that the His or His^- group of MP8 is clearly in H-bonding interaction with the peptide and/or the solvent whatever the external conditions. Moreover, the protonation and H-bonding states of the heme ligand in MP8(II) and in other HS five-coordinated hemoproteins are expected to be accessible if available X-ray crystallographic structures are used in conjunction with existing RR data. The 224-cm^{-1} frequency of neutral MP8-(II) in an aqueous CTABr solution is within the frequency range detected for several deoxymyoglobins and deoxyhemoglobins (Table IV) (Kincaid et al., 1979; Nagai et al., 1980; Desbois et al., 1979, 1981a). For these hemoproteins, the structural data indicate that the N_1 proton of the axial His could be H-bonded to a neutral backbone carbonyl group with bond lengths of 2.6–3.0 Å (Takano, 1977; Arutyunyan, 1981; Fermi et al., 1984; Arents & Love, 1989; Bolognesi et al., 1989; Evans & Brayer, 1990). A strong H-bond between the heme-bound histidylimidazole and a carbonyl peptide group is thus proposed for MP8(II) in aqueous CTABr solution at pH 7.5 (Table IV). A similar attribution may be valid for MP8(II) in the presence of NaDS where a 229-cm^{-1} band has been detected (Figure 5)(Table IV).

The 202- and 206-cm^{-1} frequencies observed in the RR spectra of neutral MP8(II) in water or in aqueous NaDS (Figures 8 (spectrum A) and 6 (spectrum A), respectively) are intermediate between the 196-cm^{-1} frequency precedently proposed as corresponding to a mode involving a "free" axial His and the 210-cm^{-1} frequency representing a weak H-bonding between the proximal (His)N_1H group and a carbonyl peptide in *Aplysia* myoglobin (Bolognesi et al., 1989) (Table IV). Two possibilities can be envisaged. A first one may correspond to an axial His without any significant H-bonding interaction, the shift from 196 to 202 or 206 cm^{-1} indicating a slight tilt of the Fe–His bond imposed by the geometries of the thioether bridges of MP8. Alternatively, a water molecule could interact with the axial His. Indeed, the less electronegative character of a water oxygen over a carbonyl oxygen makes the former atom a poorer H-bonding acceptor (Jeffrey & Saenger, 1991). Thus, the ν(FeHis) mode involving a His bound to a water molecule is expected to have a significantly lower frequency than 210–224 cm^{-1}.

The alkaline form of MP8(II) in aqueous CTABr solution exhibits the ν(FeHis)-involving mode at 243 cm^{-1}, a frequency 15 cm^{-1} lower than that observed for the mono(His^-) complex of Fe(II)–ProtoP in the same solvent conditions (258 cm^{-1})(Desbois & Lutz, 1985; Figure 10)(Table IV). The lowest frequency observed for MP8(II) is attributed to a H-bonding interaction between a proton donor and the histidinate ligand which decreases the anionic character of the latter. A peptide N–H or a hydroxyl group of Thr 19 is the most likely candidate for proton donation to the bound His^- of MP8 (Figure 9). The 243–251-cm^{-1} frequencies classify the proximal His of yeast cytochrome *c* peroxidase (CcP), horseradish peroxidase (isoenzyme C)(HRPC), and turnip peroxidases (isoenzymes 1 and 7)(TP1 and TP7, respectively) as a histidinate-like ligand (Table IV). The crystal structure of CcP shows that the carboxylate (or carboxylic) group of an Asp residue is the central element of a H-bonding network which involves the N_1 atom of the proximal His and the indole cycle of a Trp residue (Finzel et al., 1984). The frequency of the ν(FeHis) mode of CcP has been detected at 248 cm^{-1} (Dasgupta et al., 1989), in agreement with a H-bonding interaction between His and Asp. The position of the proton, however, is not determined, and the two following interactions may be considered: (His)-$N_1^-\cdots HO_2C$(Asp) or (His)$N_1H\cdots{}^-O_2C$(Asp) (Wang et al., 1990). Taking into account the 258-cm^{-1} frequency of the ν($FeHis^-$), the former structure appears to be the most likely. Such a proton location is plausible for an Im^- anion stabilized by a hydrophobic environment (Wang et al., 1990). For plant peroxidases, the ν(FeHis) mode has been detected in the 242–251-cm^{-1} region (Teraoka et al., 1983; Desbois et al., 1984b) (Table IV). Sequence alignments of HRPC, TP1, and TP7 with CcP suggest that the homologous residue of Asp 235 in CcP is Gln or Lys, Asn or Asp, and Gln or Arg, respectively (Mazza & Welinder, 1980; Welinder, 1985). The side chains of all six of these amino acid residues are good candidates for the stabilization of a His^- anion (Table IV).

MP8(II) in aqueous ethanolic solution at pH 7.5 exhibits the FeHis-involving mode at 234 cm^{-1} (Figure 6, Table IV). Under these solvent conditions, the octapeptide is expected to be structured into a helix (Fronticelli & Gold, 1976; Iyer & Acharaya, 1986). With 3–4 amino acids per helix turn, one of the two carboxylate groups of the C-terminal residue (Glu 21) could interact with the imidazole group of His 18. The 234-cm^{-1} frequency which reflects an electronegative character to the bound His should therefore correspond to a (His)$N_1H\cdots{}^-O_2C$(Glu) interaction. Another possibility is constituted by a H-bonding interaction between the (His)-N_1H and the hydroxyl group of a water or an ethanol molecule. However, the lower ability of proton acceptor of OH groups over carboxylate groups makes this possibility unlikely for a ν(FeHis) frequency at 234 cm^{-1} (Table IV). An analogous situation may be considered for cyt *c'*, for which the ν(FeHis) mode has been proposed at 232 cm^{-1} (Hobbs et al., 1990). The crystallographic data on cyt *c'* from *Rhodospirillum molischianum* revealed a heme pocket exposed to solvent and without any electronegative group able to form a strong H-bond with the axial histidylimidazole (Weber et al., 1981). An alternative interpretation, by Moore et al. (1985), has proposed that this axial His, under a deprotonated state, could interact with a positively charged guanidium group from an arginine side chain located four residues after this histidinate residue. If the assignment of the 232-cm^{-1} band were correct, this latter interpretation should be favored (Table IV).

Relations between Proximal Protein Structure and Biological Activity of Heme. The preceding discussions indicate that the solvation variations around MP8 provoke structural

modifications of the peptide structure and thus changes in the microenvironment of the proximal His. These effects influence the chemical properties of the heme moiety. In particular, a strong H-bonding or a deprotonation at the (His)N_1H decreases the redox potential of heme, stabilizing the ferric oxidation state, as well as decreases the heme reactivity for exogenous ligands (Nappa et al., 1977; Doeff et al., 1983; Quinn et al., 1983). Table IV lists the frequency of the ν-(FeHis)-involving mode of a series of hemoproteins which are oxygen carriers or peroxidases. The solvent dependence of the corresponding mode of MP8 suggests that this hemopeptide could act as a mini-myoglobin (for example in aqueous CTABr at pH 7.5) or as a mini-peroxidase (in aqueous EtOH at pH 7.5 or in alkaline water). This latter suggestion is supported by the fact that the peroxidatic activity of MP8(III) in water is increased by raising the pH or by addition of alcohol (Baldwin et al., 1985).

Conclusion. The present study has identified a series of RR modes intrinsic to heme *c*. These data are expected to be useful to monitor the heme structure as well as the bonding state of the axial histidine in reduced cyt *c'*. In particular, the ca. 150-mV variability of the redox potential of cyt *c'* may reside either on various degrees of H-bonding between an axial histidinate heme ligand and the protein and/or on different heme exposures to solvent (Weber et al., 1981; Moore et al., 1985). A careful investigation of the low-frequency RR modes of these hemoproteins will be of extreme importance in elucidating this problem. Finally, it is expected that the MP8 structural model may further facilitate the development of a detailed understanding of the influence of the proximal heme–His–peptide interactions on the determination and regulation of a particular biological function.

ACKNOWLEDGMENT

Helpful comments from Dr. T. A. Mattioli are gratefully acknowledged.

REFERENCES

Abe, M., Kitagawa, T., & Kyogoku, Y. (1978) *J. Chem. Phys. 69*, 4526–4534.

Arents, G., & Love, W. E. (1989) *J. Mol. Biol. 210*, 149–161.

Argade, P., Sassaroli, M., Rousseau, D. L., Inubushi, T., Ikeda-Saito, M., & Lapidot, A. (1984) *J. Am. Chem. Soc. 106*, 6593–6596.

Aron, J., Baldwin, D. A., Marques, H. M., Pratt, J. M., & Adams, P. A. (1986) *J. Inorg. Biochem. 27*, 227–243.

Arutyunyan, E. G. (1981) *Mol. Biol. (Moscow) 15*, 27–44.

Baldwin, D. A., Marques, H. M., & Pratt, J. M. (1986) *FEBS Lett. 183*, 309–312.

Bartsch, R. G. (1978) in *The Photosynthetic Bacteria* (Clayton, R. K., & Sistrom, W. R., Eds.) Chapter 13, pp 249–280, Plenum Publishing Co., New York.

Bolognesi, M., Onesti, S., Gatti, G., Coda, A., Ascenzi, P., & Brunori, M. (1989) *J. Mol. Biol. 205*, 529–544.

Brautigan, D. L., Feinberg, B. A., Hoffman, B. M., Margoliash, E., Peisach, J., & Blumberg, W. E. (1977) *J. Biol. Chem. 252*, 574–582.

Bushnell, G. W., Louie, G. V., & Brayer, G. D. (1990) *J. Mol. Biol. 214*, 585–595.

Cartling, B. (1983) *Biophys. J. 43*, 191–205.

Chaudhury, N. K., Saini, G. S. S., & Verma, A. L. (1992) *Spectrochim. Acta 48*, 1589–1599.

Choi, S., Spiro, T. G., Langry, K. C., Smith, K. M., Budd, D. L., & La Mar, G. N. (1982) *J. Am. Chem. Soc. 104*, 4345–4351.

Choi, S., Lee, J. J., Wei, Y. H., & Spiro, T. G. (1983) *J. Am. Chem. Soc. 105*, 3692–3707.

Dasgupta, S., Rousseau, D. L., Anni, H., & Yonetani, T. (1989) *J. Biol. Chem. 264*, 654–662.

Del Bene, J. E., & Cohen, I. (1978) *J. Am. Chem. Soc. 100*, 5285–5290.

Desbois, A., & Lutz, M. (1981) *Biochim. Biophys. Acta 671*, 168–176.

Desbois, A., & Lutz, M. (1985) in *Spectroscopy of Biological Molecules* (Alix, A. J. P., Bernard, L., & Manfait, M., Eds.) pp 342–344, J. Wiley and Sons, Chichester, U.K.

Desbois, A., & Lutz, M. (1992) *Eur. Biophys. J. 20*, 321–335.

Desbois, A., Lutz, M., & Banerjee, R. (1979) *Biochemistry 18*, 1510–1518.

Desbois, A., Lutz, M., & Banerjee, R. (1981a) *Biochim. Biophys. Acta 671*, 177–183.

Desbois, A., Momenteau, M., Loock, B., & Lutz, M. (1981b) *Spectrosc. Lett. 14*, 257–269.

Desbois, A., Henry, Y., & Lutz, M. (1984a) *Biochim. Biophys. Acta 785*, 148–160.

Desbois, A., Mazza, G., Stetzkowski, F., & Lutz, M. (1984b) *Biochim. Biophys. Acta 785*, 161–176.

Desbois, A., Tegoni, M., Gervais, M., & Lutz, M. (1989) *Biochemistry 28*, 8011–8022.

Dill, K. A. (1990) *Biochemistry 29*, 7133–7155.

Doeff, M. M., Sweigart, D. A., & O'Brien, P. (1983) *Inorg. Chem. 22*, 851–852.

Ehrenberg, A., & Theorell, H. (1955) *Acta Chem. Scand. 9*, 1193–1205.

Evans, S. V., & Brayer, G. D. (1990) *J. Mol. Biol. 213*, 885–897.

Fermi, G., Perutz, M. F., Shaanan, B., & Fourme, R. (1984) *J. Mol. Biol. 75*, 159–174.

Finzel, B. C., Poulos, T. L., & Kraut, J. (1984) *J. Biol. Chem. 259*, 13027–13036.

Fronticelli, R., & Gold, R. (1976) *J. Biol. Chem. 251*, 4968–4972.

Greenwood, C., Foote, N., Peterson, J., & Thomson, A. J. (1984) *Biochem. J. 223*, 379–391.

Harbury, H. A., & Loach, P. A. (1960a) *J. Biol. Chem. 235*, 3640–3645.

Harbury, H. A., & Loach, P. A. (1960b) *J. Biol. Chem. 235*, 3646–3653.

Harbury, H. A., Cronin, J. R., Fanger, M. W., Hettinger, T. P., Murphy, A. J., Myer, Y. P., & Vinogradov, S. N. (1965) *Proc. Natl. Acad. Sci. U.S.A. 54*, 1658–1664.

Hildebrandt, P., Pielak, G. J., & Williams, R. J. P. (1991) *Eur. J. Biochem. 201*, 211–216.

Hobbs, J. D., Larsen, R. W., Meyer, T. E., Hazard, J. H., Cusanovich, M. A., & Ondrias, M. R. (1990) *Biochemistry 29*, 4166–4174.

Hori, H., & Kitagawa, T. (1980) *J. Am. Chem. Soc. 102*, 3608–3613.

Ikeda-Saito, M., Kitagawa, T., Iizuka, T., & Kyogoku, Y. (1975) *FEBS Lett. 50*, 233–235.

Iyer, K. S., & Acharaya, A. S. (1986) *Proc. Natl. Acad. Sci. U.S.A. 84*, 7014–7018.

Jeffrey, G. A., & Saenger, W. (1991) in *Hydrogen Bonding in Biological Structures*, pp 3–94, Springer Verlag, Berlin.

Jehanli, A. M. T., Stotter, D. A., & Wilson, M. T. (1976) *Eur. J. Biochem. 71*, 613–616.

Kassner, R. J. (1973) *J. Am. Chem. Soc. 95*, 2674–2677.

Kincaid, J., Stein, P., & Spiro, T. G. (1979) *Proc. Natl. Acad. Sci. U.S.A. 76*, 549–552, 4156.

Kitagawa, T., & Ozaki, Y. (1987) *Struct. Bonding (Berlin) 64*, 71–114.

Kitagawa, T., Kyogoku, Y., Iizuka, T., Ikeda-Saito, M., & Yamanaka, T. (1975) *J. Biochem. 78*, 719–728.

Kitagawa, T., Ozaki, Y., Kyogoku, Y., & Horio, T. (1977) *Biochim. Biophys. Acta 495*, 1–11.

Kitagawa, T., Nagai, K., & Tsubaki, M. (1979) *FEBS Lett. 104*, 376–378.

Lemberg, R., & Barrett, J. (1973) in *Cytochromes*, pp 122–216, Academic Press, London.

Leondiadis, L., Momenteau, M., & Desbois, A. (1992) *Inorg. Chem. 31*, 4691–4696.
Li, X.-Y., Czernuszewicz, R. S., Kincaid, J. R., Su, Y. O., & Spiro, T. G. (1990a) *J. Phys. Chem. 94*, 31–47.
Li, X.-Y., Czernuszewicz, R. S., Kincaid, J. R., Stein, P., & Spiro, T. G. (1990b) *J. Phys. Chem. 94*, 47–61.
Maeda, H., Nizu, T., Fukada, K., & Ikeda, S. (1988) *Macromolecules 21*, 1154–1158.
Margoliash, E., & Schejter, A. (1966) *Adv. Protein Chem. 21*, 113–286.
Mashiko, T., Marchon, J.-C., Musser, D. J., Reed, C. A., Kastner, M. E., & Scheidt, W. R. (1979) *J. Am. Chem. Soc. 101*, 3653–3655.
Mattice, W. L. (1989) *Annu. Rev. Biophys. Biophys. Chem. 18*, 93–111.
Mazza, G., & Welinder, K. G. (1980) *Eur. J. Biochem. 108*, 481–489.
Meyer, T. E., & Kamen, M. D. (1982) *Adv. Protein Chem. 35*, 105–212.
Mincey, T., & Traylor, T. G. (1979) *J. Am. Chem. Soc. 101*, 765–766.
Moore, G. R., & Williams, R. J. P. (1980) *Eur. J. Biochem. 103*, 533–541.
Moore, G. R., Williams, R. J. P., Peterson, J., Thomson, A. J., & Mathews, F. S. (1985) *Biochem. Biophys. Acta 829*, 83–96.
Nagai, K., Kitagawa, T., & Morimoto, H. (1980) *J. Mol. Biol. 136*, 271–289.
Nappa, M., Valentine, J. S., & Snyder, P. A. (1977) *J. Am. Chem. Soc. 99*, 5799–5800.
Parthasarathi, N., Hanson, C., Yamagushi, S., & Spiro, T. G. (1987) *J. Am. Chem. Soc. 109*, 3865–3871.
Quinn, R., Strouse, C. E., & Valentine, J. S. (1983) *Inorg. Chem. 22*, 3934–3940.
Roberts, J. D., Yu, C., Flanagan, C., & Birdseye, T. R. (1982) *J. Am. Chem. Soc. 104*, 3945–3949.
Rousseau, D. L. (1981) *J. Raman Spectrosc. 10*, 94–99.
Sarkar, P. K., & Doty, P. (1966) *Proc. Natl. Acad. Sci. U.S.A. 55*, 981–989.
Schejter, A., Aviram, I., & Goldkorn, T. (1982) in *Electron Transport and Oxygen Utilization* (Ho, C., Ed.) pp 95–99, Macmillan Press, London.
Senn, H., & Wüthrich, K. (1985) *Q. Rev. Biophys. 18*, 111–134.
Shelnutt, J. A., Rousseau, D. L., Dethmers, J. K., & Margoliash, E. (1981) *Biochemistry 20*, 6435–6497.
Simpkin, D., Palmer, G., Devlin, F. J., McKenna, M. C., Jensen, G. M., & Stephens, P. J. (1989) *Biochemistry 28*, 8033–8039.
Smith, M., & McLendon, G. (1981) *J. Am. Chem. Soc. 103*, 4912–4921.
Spiro, T. G. (1985) *Adv. Protein Chem. 34*, 111–159.
Spiro, T. G., & Burke, J. M. (1976) *J. Am. Chem. Soc. 98*, 5482–5489.
Stein, P., Mitchell, M., & Spiro, T. G. (1980) *J. Am. Chem. Soc. 102*, 7795–7797.
Stellwagen, E. (1978) *Nature 275*, 73–74.
Stavrov, S. S. (1993) *Biophys. J.*, submitted for publication.
Strekas, T. C., & Spiro, T. G. (1972) *Biochim. Biophys. Acta 278*, 188–192.
Strekas, T. C., & Spiro, T. G. (1974) *Biochim. Biophys. Acta 351*, 237–245.
Takano, T. (1977) *J. Mol. Biol. 110*, 537–568.
Teraoka, J., & Kitagawa, T. (1981) *J. Biol. Chem. 256*, 3969–3977.
Teraoka, J., Job, D., Morita, Y., & Kitagawa, T. (1983) *Biochim. Biophys. Acta 747*, 10–15.
Tuppy, H., & Paléus, S. (1955) *Acta Chem. Scand. 9*, 353–364.
Urry, D. W., & Pettigrew, J. W. (1967) *J. Am. Chem. Soc. 89*, 5276–5283.
Valentine, J. S., Sheridan, R. P., Allen, L. C., & Kahan, P. C. (1979) *Proc. Natl. Acad. Sci. U.S.A. 76*, 1009–1013.
Vickery, L., Nozawa, T., & Sauer, K. (1976) *J. Am. Chem. Soc. 98*, 351–357.
Wang, J., Mauro, J. M., Edwards, S. L., Oatley, S. J., Fishel, L. A., Ashford, V. A., Xuong, N., & Kraut, J. (1990) *Biochemistry 29*, 7160–7173.
Weber, P. C., Howard, A., Xuong, N. H., & Salemme, F. R. (1981) *J. Mol. Biol. 153*, 399–424.
Welinder, K. G. (1985) *Eur. J. Biochem. 151*, 497–504.
Wells, A. V., Sage, J. T., Morikis, D., Champion, P. M., Chiu, M. L., & Sligar, S. G. (1991) *J. Am. Chem. Soc. 113*, 9655–9660.
Wilson, M. T., Ranson, R. J., Masiakowski, P., Czarnecka, E., & Brunori, M. (1977) *Eur. J. Biochem. 77*, 193–199.
Yoshimura, T., Susuki, S., Nakahara, A., Iwasaki, H., Masuko, M., & Matsubara, T. (1985) *Biochim. Biophys. Acta 831*, 267–274.